Original Research Article

GREENHOUSE GASES SCIENCE AND TECHNOLOGY

ECO2N V2.0: A TOUGH2 fluid property module for modeling CO_2-H_2O-NACL systems to elevated temperatures of up to 300°C

Lehua Pan, Nicolas Spycher, Christine Doughty and Karsten Pruess, Lawrence Berkeley National Laboratory, University of California, Berkeley, CA, USA

Abstract: We have improved ECO2N, the TOUGH2 fluid property module of the CO_2-H_2O-NaCl system. The major enhancements include: (i) the upper temperature limit is increased from 110 to about 300°C; (ii) the thermophysical properties of the CO_2-rich phase are more accurately calculated as a non-ideal mixture of CO_2 and H_2O; (iii) the approach to calculate the specific enthalpy of dissolved CO_2 has been improved to make the code more robust in modeling phase transitions under non-isothermal conditions; and (iv) more sophisticated models for effective heat conductivity of formations saturated with supercritical CO_2 have been provided. The new module includes a comprehensive description of the thermodynamic and thermophysical properties of H_2O–NaCl–CO_2 mixtures, that reproduces fluid properties largely within experimental error for the temperature, pressure and salinity conditions $10°C < T < 300°C$, $P < 600$ bar, and salinity up to halite saturation. This includes density, viscosity, and specific enthalpy of fluid phases as functions of temperature, pressure, and composition, as well as partitioning of mass components H_2O, NaCl and CO_2 among the different phases. ECO2N with the TOUGH2 reservoir simulator can be applied to a wide range of problems in geologic sequestration of CO_2 in saline aquifers, and in enhanced geothermal reservoirs. ECO2N can describe both sub- and supercritical states of CO_2, but applications that involve subcritical conditions are limited to systems in which there is no change of phase between liquid and gaseous CO_2, and in which no mixtures of liquid and gaseous CO_2 occur. © 2016 Society of Chemical Industry and John Wiley & Sons, Ltd.

Keywords: numerical simulator; elevated temperature; fluid property; geological carbon sequestration; CO_2-brine; CO_2-based EGS

Introduction

TOUGH2/ECO2N[1–3] is a widely used numerical simulator for investigating problems involved in CO_2 geological sequestration. However, the previous version (V1.0) of ECO2N is only applicable to systems with temperature up to 110°C.[4] As a result, many problems that involve higher temperature could not be simulated by the code. Motivated by the potential for enhanced geothermal systems (EGS) operating with CO_2, and CO_2 geologic storage at temperatures above 100°C,

Correspondence to: Lehua Pan, Energy Geosciences Division, Lawrence Berkeley National Laboratory, University of California, One Cyclotron Road, Berkeley, CA 94720, USA. E-mail: lpan@lbl.gov

Received March 3, 2016; revised June 27, 2016; accepted July 4, 2016

Published online at Wiley Online Library (wileyonlinelibrary.com). DOI: 10.1002/ghg.1617

Spycher and Pruess[5] developed new mutual solubility correlations for higher temperatures. ECO2N V2.0 is an enhanced version of ECO2N V1.0 that inherits all the capabilities of ECO2N V1.0 and expands the applicable temperature range up to about 300°C by incorporating the newly developed mutual solubility correlations for higher temperature.[5] The fluid property module can be used to model non-isothermal multiphase flow in the system H_2O-NaCl-CO_2. TOUGH2/ECO2N V2.0 represents fluids as consisting of two phases: a water-rich aqueous phase, hereafter referred to as aqueous or 'liquid'; and a CO_2-rich phase, hereafter referred to as 'gas'. In addition, solid salt may also be present. The only chemical reactions modeled by ECO2N V2.0 are equilibrium phase partitioning of water and carbon dioxide between the liquid and gas phases, and precipitation and dissolution of solid salt. The partitioning of H_2O and CO_2 between liquid and gas phases is modeled as a function of temperature, pressure, and salinity, using the recently developed correlations of Spycher and Pruess.[5,6] Dissolution and precipitation of salt are treated by means of local equilibrium solubility. Associated changes in fluid porosity and permeability may also be modeled. All phases – gas, liquid, solid – may appear or disappear in any grid block during the course of a simulation. Thermodynamic conditions covered include a temperature range from about 10°C to 300°C (approximately), pressures up to 600 bar, and salinity up to NaCl (halite) saturation. Note that ECO2N can describe both subcritical and supercritical states of CO_2, but applications that involve subcritical conditions are limited to systems in which there is no change of phase between liquid and gaseous CO_2, and in which no mixtures of liquid and gaseous CO_2 occur. For those cases, a user may use the fluid property module ECO2M[7] instead.

ECO2N V2.0 uses the same framework for describing the thermophysical status of H_2O-NaCl-CO_2 systems as its preceding version (Table 1). This paper will only describe the new enhancements which are not available in V1.0.

Code enhancements

Extended CO2-H2O solubility model

The upper temperature limit of the H_2O-CO_2 mutual solubility model has been extended from 110°C to about 300°C. In particular, partitioning among co-existing aqueous and gas phases is calculated based on the correlations developed by Spycher and Pruess[6] for the low temperature range (<99°C) and Spycher and Pruess[5] for the high temperature range (109°C to ~300°C). At temperatures between 99°C and 109°C, a cubic function is applied to interpolate both the equilibrium mass fraction of CO_2 in the aqueous phase and the equilibrium mass fraction of H_2O in the gas (CO_2-rich) phase. This approach guarantees a smooth transition between the low temperature and the high temperature ranges such that both the solubility function and its first derivative are continuous (Fig. 1).

Non-ideal gas (CO_2-rich) phase properties

Unlike ECO2N V1.0, which approximates the gas phase properties with the properties of pure CO_2, V2.0 calculates the actual properties of non-ideally mixed gas phase of CO_2 and H_2O. In the gas phase, the CO_2 behaves either as a liquid, gas, or as a supercritical fluid while the water could be considered as water vapor. However, its properties tend to deviate from 'vapor-like' and approach 'liquid-like' values as the gas phase pressure increases.[8] At elevated pressures, the H_2O partial pressure in the gas phase can be well above the saturation pressure of pure H_2O, $P_{sat}(T)$. To properly model the effects of H_2O on the properties of the CO_2-rich phase, two new approaches have been implemented in ECO2N V2.0: (i) The use of simple, smooth mixing functions of pure component properties (default option, IE(16) = 0), and (ii) the direct use of the cubic EOS implemented for solubility calculations (IE(16) = 2). For IE(16) = 1, gas phase properties are calculated as in ECO2N V1.0. The following is a brief description of the first new approach (default). The second new approach is discussed in detail by Spycher and Pruess[5,8] and will not be repeated here.

The gas phase density ρ_{gas} is calculated as a sum of the partial densities, ρ_{CO2} and ρ_{H2O}:

$$\rho_{gas} = \rho_{CO2} + \rho_{H2O} \tag{1a}$$

The partial densities are calculated as follows:

$$\rho_{CO2} = \left(1 - y_{H2O}\right) \rho_a \left(P, T\right)$$
$$\rho_{H2O} = \rho_{sv} \left(P_v, T\right) + X_L^{1.8}\, y_{H2O}\, \rho_{sL} \left(P, T\right) \tag{1b}$$

where y_{H2O} is the mole fraction of H_2O in the gas phase and X_L is taken as zero if the actual partial

Table 1. Summary of ECO2N V2.0 thermophysical capabilities.

Components: #1: water, #2: NaCl, #3: CO_2

Parameter choices

(NK, NEQ, NPH, NB)[a]

= (3, 4, 3, 6) water, NaCl, CO_2, non-isothermal (default)

= (3, 3, 3, 6) water, NaCl, CO_2, isothermal

molecular diffusion can be modeled by setting NB = 8

Primary variables

single fluid phase (only aqueous, or only gas)[b] (P, Xsm, X3, T)

P – pressure (Pa)

Xsm – NaCl salt mass fraction Xs (on the basis of a two-component, CO_2-free water-salt system), or solid NaCl saturation Ss+10

X3 – CO_2 (true) mass fraction in the aqueous phase, or in the gas phase,

in the three-component system water-salt-CO2

T – temperature (°C)

two fluid phases (aqueous and gas)[b] (P, Xsm, Sg+10, T)

P – gas phase pressure (Pa)

Xsm – NaCl salt mass fraction Xs (on the basis of a two-component, CO_2-free water-salt system), or solid saturation Ss+10

Sg – gas phase saturation

T – temperature (°C)

[a]NK – maximum number of mass components; NEQ – maximum number of equations per grid block; NPH – maximum number of active phases (including solid salt); NB – number of secondary parameters other than component mass fractions.
[b]When discussing fluid phase conditions, we refer to the potentially mobile (aqueous and gas) phases only; in all cases solid salt may precipitate or dissolve, adding another active phase to the system.

pressure of water (P_{H2O}) is equal to, or less than, the saturation pressure of pure water ($P^0{}_{sat}$) at the prevailing temperature, or as ($1 - P^0{}_{sat}/P_{H2O}$) if $P_{H2O} > P^0{}_{sat}$ (X_L could be viewed as a factor proportional to the fraction of liquid-like H_2O within the total H_2O component). ρ_a and ρ_{sL} are the densities of pure CO_2 and H_2O liquid, respectively, at the prevailing temperature and pressure, whereas ρ_{sv} is the density of pure H_2O vapor at the prevailing temperature but corresponding to P_v ($= \min(P_{H2O}, P^0{}_{sat})$). The calculated densities compare well with the experimental data reported in the literature for various composition, pressure, and temperature (Fig. 2).

The gas phase specific enthalpy is also calculated as a sum of contributions from both components plus an empirical mixing heat term:

$$h_{gas} = y_{H2O}\, h_{H2O} + \left(1 - y_{H2O}\right) h_{CO2} + y_{H2O}\left(\frac{P}{\rho_{gas}} - \frac{P_{H2O}}{\rho_{H2O}}\right) \qquad (2)$$

where h_{CO2} is the specific enthalpy of the CO_2 component, and h_{H2O} is the specific enthalpy of the H_2O component, which is calculated as:

$$h_{H2O} = (1 - X_L)\, u_{sv} + X_L\, u_{sL} + \frac{P_{H2O}}{\rho_{H2O}} \qquad (3)$$

where u_{sv} and u_{sL} are the specific enthalpies of water vapor and liquid water, respectively. The calculated enthalpy values compare well with the experimental data reported in the literature for various compositions, pressures, and temperatures (Fig. 3). Note that the same reference state (i.e., the internal energy of saturated liquid water equals zero at the triple point of pure water) is used in ECO2N V2.0 for both components. As a result, the enthalpy of the CO_2 component in V2.0 is smaller than that in V1.0 by a constant (302 192 J/kg) (unless IE(16) = 1 – when the ECO2N V1.0 formulation for water/CO2 properties is used the reference state is unchanged from V1.0).

The viscosity of the gas phase is calculated based on the fluidity method proposed by Davidson.[16]

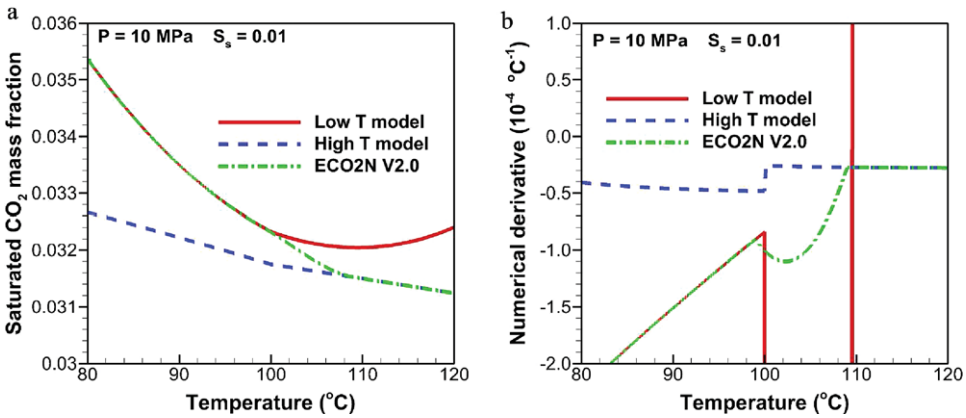

Figure 1. Transition between low temperature model (<99°C) and high temperature model (>109°C). (a) Computed dissolved CO_2 mass fraction (at saturation) as a function of temperature; (b) the numerical derivative of the dissolved CO_2 mass fraction with respect to temperature ($\Delta T = 1E{-}8°C^{-1}$). 'Low T model' indicates the mutual solubility model developed by Spycher and Pruess,[6] whereas 'High T model' indicates the mutual solubility model for higher temperatures by Spycher and Pruess.[5] 'ECO2N V2.0' indicates the combined model implemented in ECO2N V2.0.

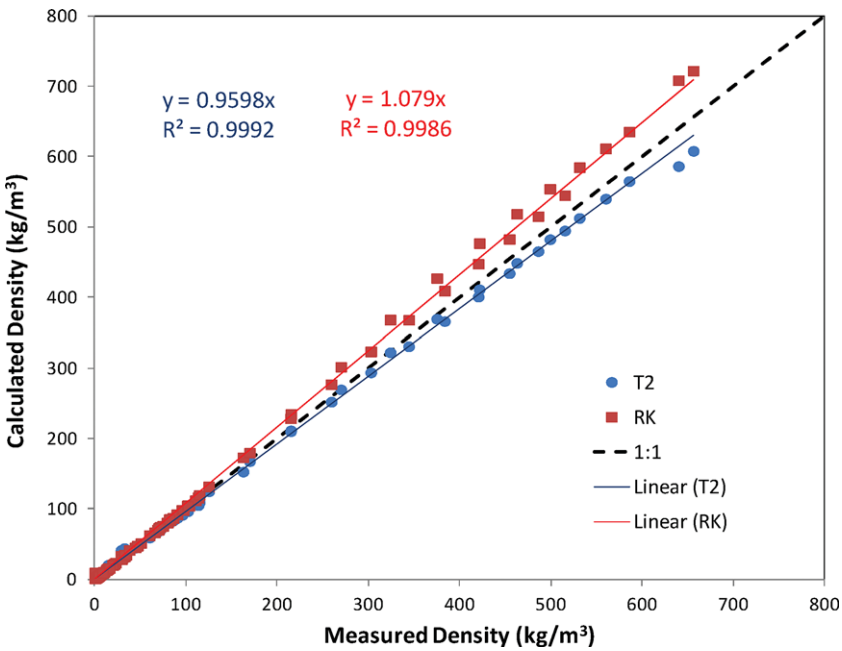

Figure 2. Comparison of computed densities of the gas phase against the experimental data reported in the literature.[9–13] T2 indicates the default model (Eqn (1)) while RK indicates the alternative model (IE(16) = 2).

Non-iterative calculation of specific enthalpy of dissolved CO_2 under single-phase aqueous conditions

In the previous version of ECO2N (V1.0), the specific enthalpy of dissolved CO_2 for the entire range of CO_2 mass fraction (the 3rd primary variable, X3) can be summarized (the subscript g or l was dropped for simplicity)as:

$$h_{CO2,aq}(T, P, X_s) = \begin{cases} h_a(T, P) + h_{dis}(T, X_s) & X3 \geq X_{CO2,eq} \\ h_a(T, P_{X3}) + h_{dis}(T, X_s) & X3 < X_{CO2,eq} \end{cases} \quad (4)$$

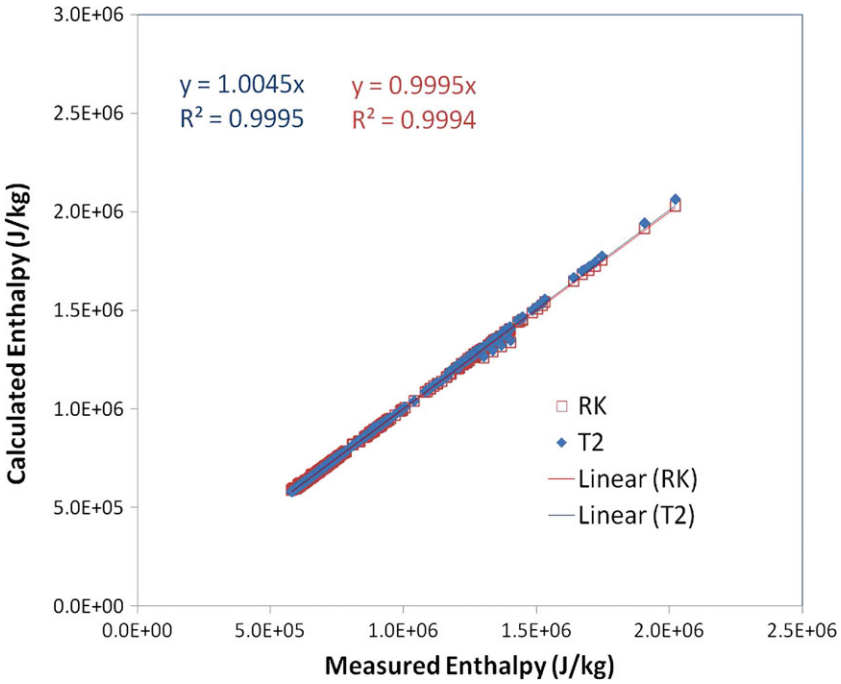

Figure 3. Comparison of computed specific enthalpy of the gas phase against the experimental data reported in the literature.[11,14,15] T2 indicates the default model while RK indicates the alternative model (IE(16) = 2).

where h_{dis} is the heat of dissolution of CO_2. $X_{CO2,eq}$ is the equilibrium mass fraction of CO_2 in the aqueous phase at given P, T, and X_s above which free gas occurs. The specific enthalpy of CO_2, $h_a(T, P)$, is calculated as a function of temperature and pressure through bivariate interpolation from a tabulation of Altunin's[17] correlation. P_{X3} is the saturation pressure corresponding to the given CO_2 mass fraction in the aqueous phase at given T, which is obtained by inversion of the solubility correlation using an iterative procedure. However, this approach was found often to suffer convergence problems for non-isothermal simulations, especially during appearance or disappearance of a free CO_2 phase. The reason is that the specific enthalpy of dissolved CO_2 calculated using Eqn (4) does not have a continuous first derivative at the phase change line, which could lead to an inaccurate Jacobian matrix and cause convergence problems when the system is close to a phase change. Figure 4 shows an example contour map of the specific enthalpy of dissolved CO_2 (excluding h_{dis} for simplicity) at given temperature (40°C) and salinity (0.01). Above the phase change line, the specific enthalpy only depends on the pressure. Below the phase change line, it only depends on the mass fraction X3.

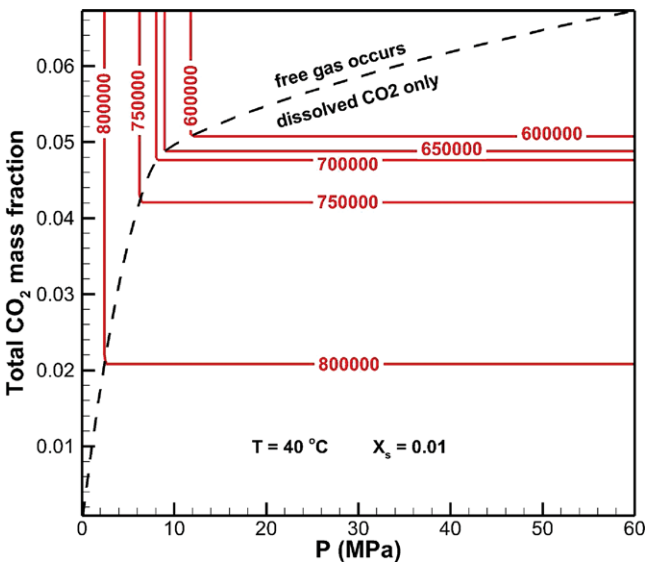

Figure 4. Contours of the specific enthalpy, $h_{CO2,aq} - h_{dis}$, (J/kg) of dissolved CO_2 (red lines) as a function of total CO_2 mass fraction X3 and pressure at a given temperature (40°C) and salt mass fraction (0.01) as calculated in ECO2N V1.0. The phase change line (black dashed line) is calculated using the correlations developed by Spycher and Pruess.[6] The specific enthalpy is continuous at the phase change line, but its partial derivative with respective to either pressure or CO_2 mass fraction is not.

Although $h_{CO2,aq}$ is continuous across the phase change line, the partial derivative of $h_{CO2,aq}$ with respect to X3 is non-zero when approaching the line from below but is zero when approaching the line from above. Similar discontinuities can be found in the partial derivatives with respect to other variables (e.g. P, T, or Xs).

In ECO2N V2.0, we use a modified approach to calculate the enthalpy of dissolved CO_2 so that its derivatives with respect to either primary variable are continuous across the phase change line. We evaluate the specific enthalpy of the dissolved CO_2 for single-phase aqueous conditions as a non-linearly scaled value of its counterpart under two-phase conditions.

$$h_{CO2,aq}(T, P, X_s) = \begin{cases} h_a(T,P) + h_{dis}(T,X_s) & X3 \geq X_{CO2,eq} \\ h_a(T,P)\, f(X3) + h_{dis}(T,X_s) & X3 < X_{CO2,eq} \end{cases} \quad (5)$$

where the scaling function f(X3) is defined as follows:

$$f(X3) = 2 - \cos\left[3\pi\left(X_{CO2,eq} - X3\right)\right] \quad (6)$$

As a result, ECO2N V2.0 does not suffer the convergence problems caused by the discontinuous first derivatives of the specific enthalpy across the CO_2 saturation line and appears to be more robust than V1.0 especially for non-isothermal applications, even though the calculated enthalpies of dissolved CO_2 are practically identical in V2.0 and V1.0 (Fig. 5). The iterative calculation to obtain P_{X3} is no longer needed in V2.0 because f(X3) is a direct function of the third primary variable X3.

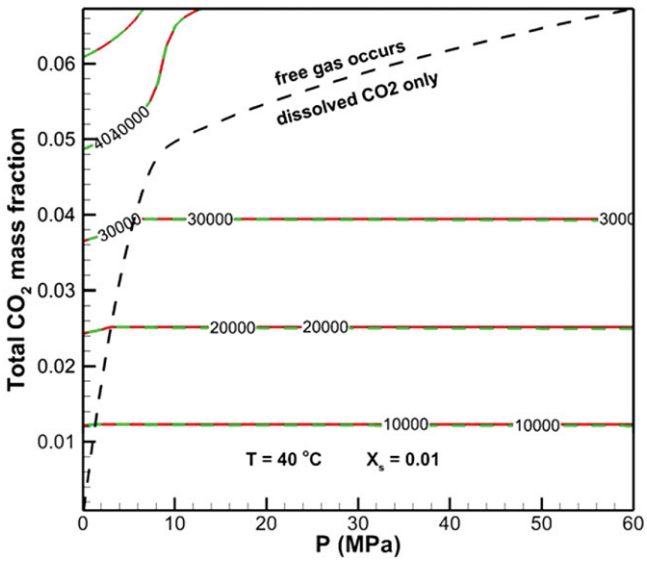

Figure 5. Contours of the scaled specific enthalpy of dissolved CO_2, $\min(X3, X_{CO2,eq})(h_{CO2,aq} - h_{dis})$, (J/kg) as a function of total CO_2 mass fraction X3 and pressure at a given temperature (40°C) and salt mass fraction (0.01). V1.0 is the red lines whereas V2.0 is the green dashed lines. The phase change line (black dashed line) is calculated using the correlations developed by Spycher and Pruess.[6]

Sophisticated models for effective heat conductivity

Two more sophisticated models for effective heat conductivity of formations containing CO_2 have been provided (optional, require some modifications to the TOUGH2 core code) for further improvement of the simulation of CO_2-H_2O-NaCl systems. These are useful because the thermal conductivity of CO_2 varies greatly depending on its occurrence as a gas, a liquid, or a supercritical fluid (Fig. 6). The first new model employs expressions for CO_2[18] and brine[19,20] thermal conductivity as a function of pressure and temperature, then uses the effective medium theory of Zimmerman[21] to combine them with the user-specified rock thermal conductivity to get an effective thermal conductivity for the grid block. The second new model retains the original TOUGH feature of the user specifying the effective thermal conductivity for liquid (aqueous) and gas (CO_2)-saturated conditions, but modifies the CO_2-saturated thermal conductivity in proportion to CO_2 density. The details of models are described in the users' guide.[22]

Example problems

Non-isothermal radial flow from a CO_2 injection well

This is a variation of the test problem #3 in a code inter-comparison project.[23,24] The variation is that the flow process is non-isothermal here, i.e., colder CO2 is injected into a warmer saline aquifer. The problem is formulated as follows. A CO_2 injection well fully penetrates a homogeneous, isotropic, infinite-acting aquifer of 100 m thickness (Fig. 7), at conditions of 120 bar pressure, 45°C temperature, and a salinity of 15% by weight. Colder CO_2 (at 35°C) is injected uniformly at a constant rate of 100 kg/s.

Figure 8 shows the simulated results in terms of the 'similarity variable' R^2/t obtained by O'Sullivan.[25] Three distinct regions of gas saturation (Fig. 8(b)), solid salt saturation (Fig. 8(c)), CO_2 mass fraction in

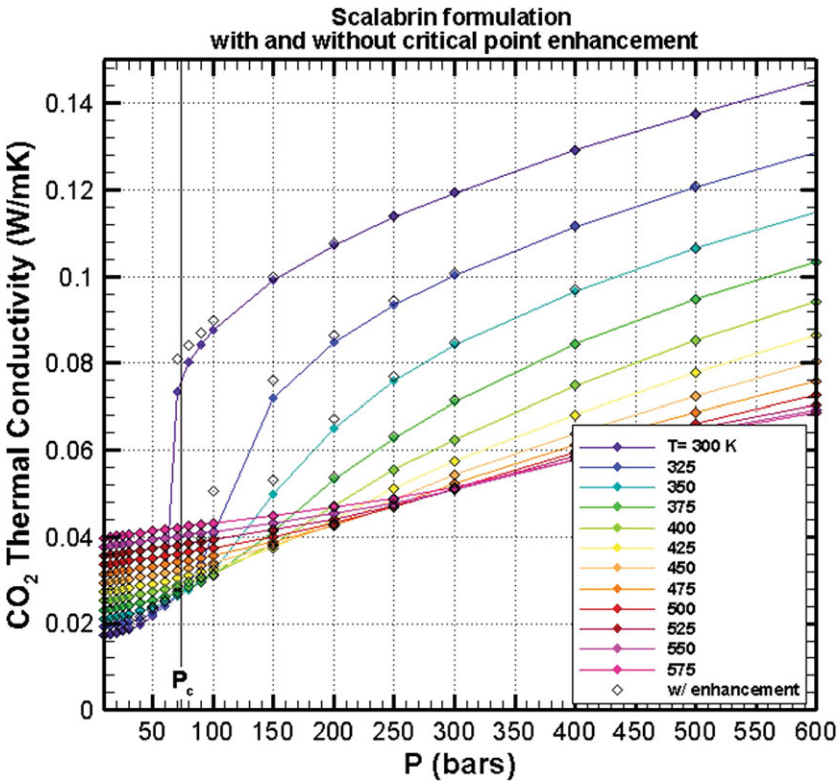

Figure 6. CO_2 thermal conductivity as a function of temperature and pressure.

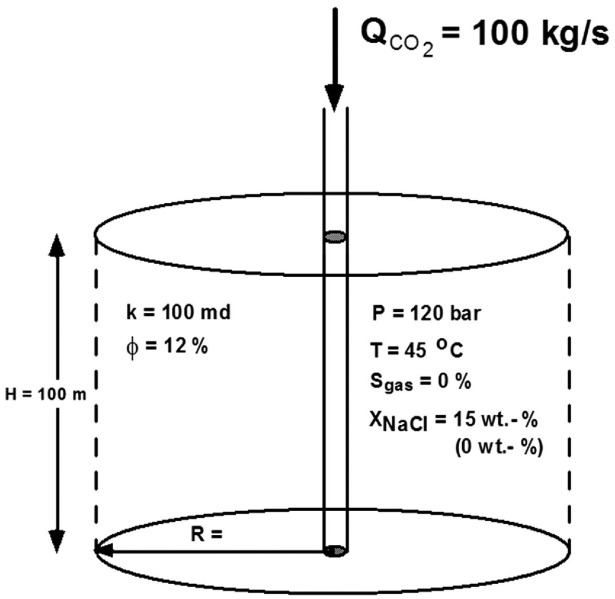

Figure 7. Schematic of radial flow sample problem.

liquid (Fig. 8(d)), and NaCl mass fraction in liquid (Fig. 8(e)), can be found in this non-isothermal CO_2 injection process, namely, dry-out zone, two-phase zone, and single aqueous phase zone. The two-phase zone consists of two sub-regions. In the sub-region near the dry end, the CO_2 mass fraction is higher than near the wet end. The dividing point corresponds to the temperature front formed during injection of colder CO_2 into a warm aquifer (Fig. 9). Behind the front, the temperature is low and more CO_2 can be dissolved in water, while higher temperature and less dissolved CO_2 exist ahead of the front. Interestingly, the temperature in the dry sub-region is slightly lower than the injection temperature, implying that the cooling effect due to water evaporation into the flowing CO_2 is dominating behind the temperature front, whereas the temperature in the wet sub-region is slightly higher than the ambient aquifer temperature, implying that the heating effect due to dissolution of CO_2 into water is dominating ahead of the temperature front (Fig. 8(f)). Note from the temperature profile (Fig. 8(f)) that by accounting for the effects of water in the CO_2-rich phase in the enthalpy calculation, the water-evaporation induced temperature drop predicted by ECO2N V2.0 is smaller than that obtained by the case using pure CO_2 properties for the gas phase (V1.0).

The agreement between ECO2N V2.0 and ECO2N V1.0 is excellent, except for the differences noted, based on more complete physics.

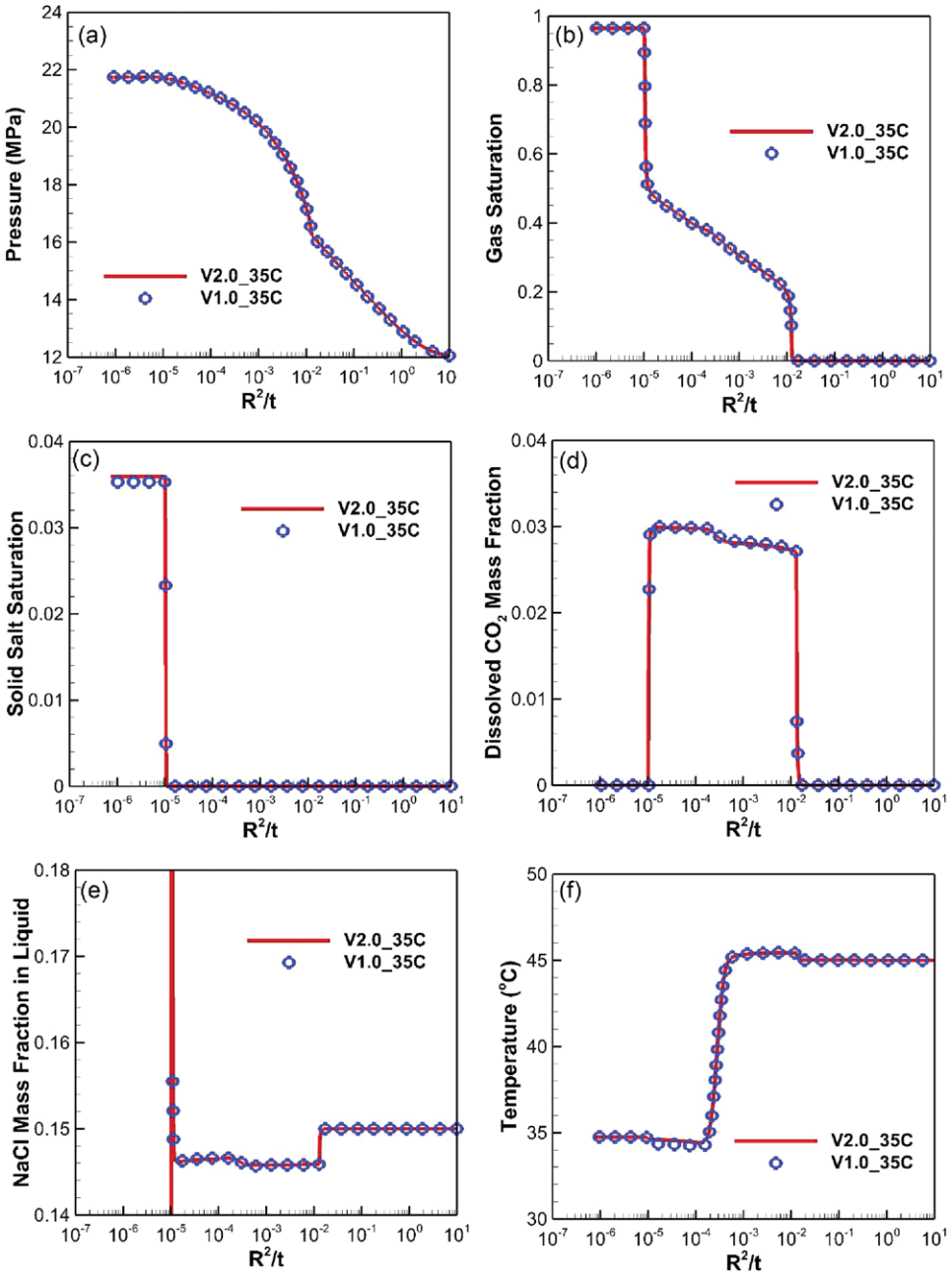

Figure 8. Simulated pressures (a), gas saturation (b), solid salt saturation (c), dissolved CO_2 mass fraction (d), dissolved NaCl mass fraction (e), and temperature (f) as a function of the similarity variable R^2/t, where R is the radial distance from the well and t is time. The solid red lines represent the results simulated by the new code (ECO2N V2.0), while the blue symbols represent the results simulated by ECO2N V1.0. All results are time series of data for a grid block at a radial distance of R = 25.25 m.

GCS/GHE with a double-porosity reservoir

In this problem, we consider an injection-well/production-well pair representing a 1/8 symmetry element of a five-spot pattern (Fig. 10(a)) that makes up a geothermal heat extraction (GHE) system combined with geological carbon sequestration (GCS). The geothermal reservoir we consider here is an idealized 100 m thick double porosity reservoir,[26] whose parameters are shown in Tables 2 and 3. In the double-porosity model, one continuum represents the

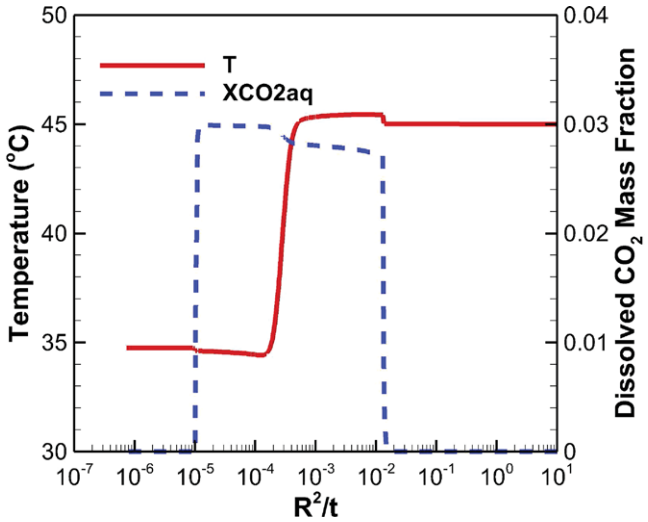

Figure 9. Simulated temperature and dissolved CO_2 mass fraction as a function of the similarity variable (non-isothermal radial flow). The solid red line represents temperature while the blue dashed line represents the mass fraction of the dissolved CO_2 in aqueous phase. All results are time series of data for a grid block at a radial distance of R = 25.25 m.

Table 2. Parameters of the double porosity model.

Parameter	Value
Percentage of fracture pore space (%)	20
Permeability of the fracture continuum (m^2)	2E−14
Permeability of the matrix (m^2)	2E−17
Percentage of matrix pore space (%)	80
Fracture/matrix interface area per unit volume (m^2/m^3)	0.2
Characteristic fracture/matrix distance (m)	5.0

higher permeability regions (fractures) through which global flow occurs, while the other represents lower permeability regions (rock matrix), that may exchange fluid and heat with the high-permeability domain locally. The reservoir is assumed to be initially filled with pure CO_2 in the fractures and pure water in the matrix, under the same hydrostatic pressure (29.15 MPa) and temperature (152.2°C). Because the fracture continuum makes up 20% of the reservoir, this initial condition is equivalent to an initial bulk gas saturation of 20%.

A 2D, irregular, dual-continuum grid was created to represent the reservoir, in which each continuum is represented by a 2D mesh having the same geometry (Fig. 10(b)), except that the matrix continuum mesh does not have global flow connections. The two overlapping meshes are connected locally. In other words, fluid can flow from the injection well to the production well through the fracture continuum only, whereas the matrix continuum plays a passive role through mass and heat exchange with the fractures. Grid resolution varies from 0.1 m near the wells to 50 m at far field to capture the important details of the flow field. Both the injection and the production wells are fully perforated in the reservoir (connected to the fracture continuum only). The parameters for the double porosity model used in this study are shown in Table 2.

With the exception of capillary strength, the parameters for relative permeability and capillary functions are the same for both continua, as shown in Table 3.

No-flow boundaries are assigned on all sides except for conductive heat flow through the reservoir/basement rock interface, which is calculated using a semi-analytical solution implemented in TOUGH2.[29] Injection of CO_2 is simulated as a source term at the injection well cell with a rate of 6.25 kg/s (1/8 of 50 kg/s for the full well) at a constant temperature of 75°C. The same flow rate is assigned for the mass produced at the production well.

Figure 11 shows six snapshots of pressure change (from the initial pressure) in the fracture continuum during the production. The reservoir pressure drops quickly at early time and then slowly recovers to some degree. As a result, the pressure drop after one year is the biggest among the six snapshots. This implies that the reservoir pressure loss is mainly caused by the volume imbalance due to production of hot CO_2 and injection of cold CO_2. Such volume loss is gradually compensated by the expansion of the injected cold CO_2 with time. Figure 12 shows the temperature distribution in both continua at various times. The cold front advances with time from the injection well to the production well. There is a time-delay in the matrix continuum in such propagation, especially at early time.

Figure 13 shows three snapshots of gas saturation in each continuum during production. The gas saturation in the matrix continuum slowly increases with time as CO_2 enters from the fracture continuum. The gas saturation in the fracture continuum first drops over the entire domain and then increases near the injection well as injection continues, forming a significant gradient from the injection well to the production well. Water accumulates in the region close to the

Table 3. Other properties of the reservoir (both continua).

Parameter	Value	Note
Porosity	0.254	Uniform
Thermal conductivity	2.51 W m^{-1} K^{-1}	
Pore compressibility	10^{-10} Pa^{-1}	
Parameters for relative permeability:		
Residual gas saturation	0.01	Liquid relative permeability using van Genuchten-Mualem[27] model and gas relative permeability using Corey[28] model
m_{VG}	0.65	
Residual liquid saturation	0.05	
Saturated liquid saturation	1.0	
Parameters for capillary pressure:		
Residual liquid saturation	0.03	Capillary pressure using van Genuchten[27] model
m_{VG}	0.4118	
$1/P_0$	6.08E−5 Pa^{-1} (fracture continuum)	
	1.216E-6 Pa^{-1} (matrix continuum)	
Maximum capillary pressure	6.4×10^7 Pa	
Saturated liquid saturation	1.0	

production well (Fig. 13(e)). However, the liquid phase production rate is small for most times (Fig. 14(a)), and the CO_2 component in the total production is larger than 97% (Fig. 14(b)).

Conclusions

ECO2N V2.0 is an enhanced version of ECO2N V1.0, a fluid property module for the multiphase, multicomponent simulator TOUGH2, Version 2.1. The new code provides capabilities for modeling advective and diffusive flow and transport in multidimensional heterogeneous systems containing H_2O-NaCl-CO_2 mixtures with temperatures from ambient up to 300°C. Process capabilities include coupling between fluid and heat flow, partitioning of H_2O and CO_2 among different phases, and precipitation/dissolution of solid

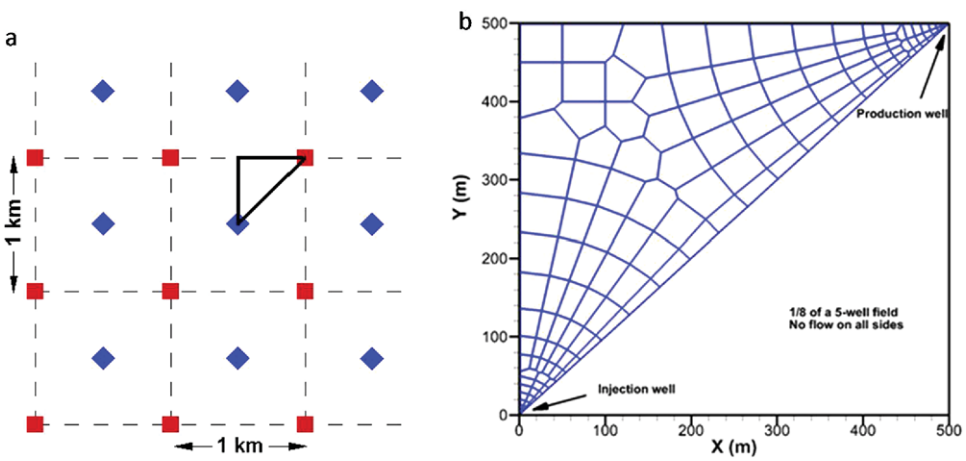

Figure 10. (a) Diagram of five-spot pattern of geothermal wells (blue-injector; red-producer); (b) map view of the numerical grid used in the simulation. Finer grid resolution is used near the two wells.

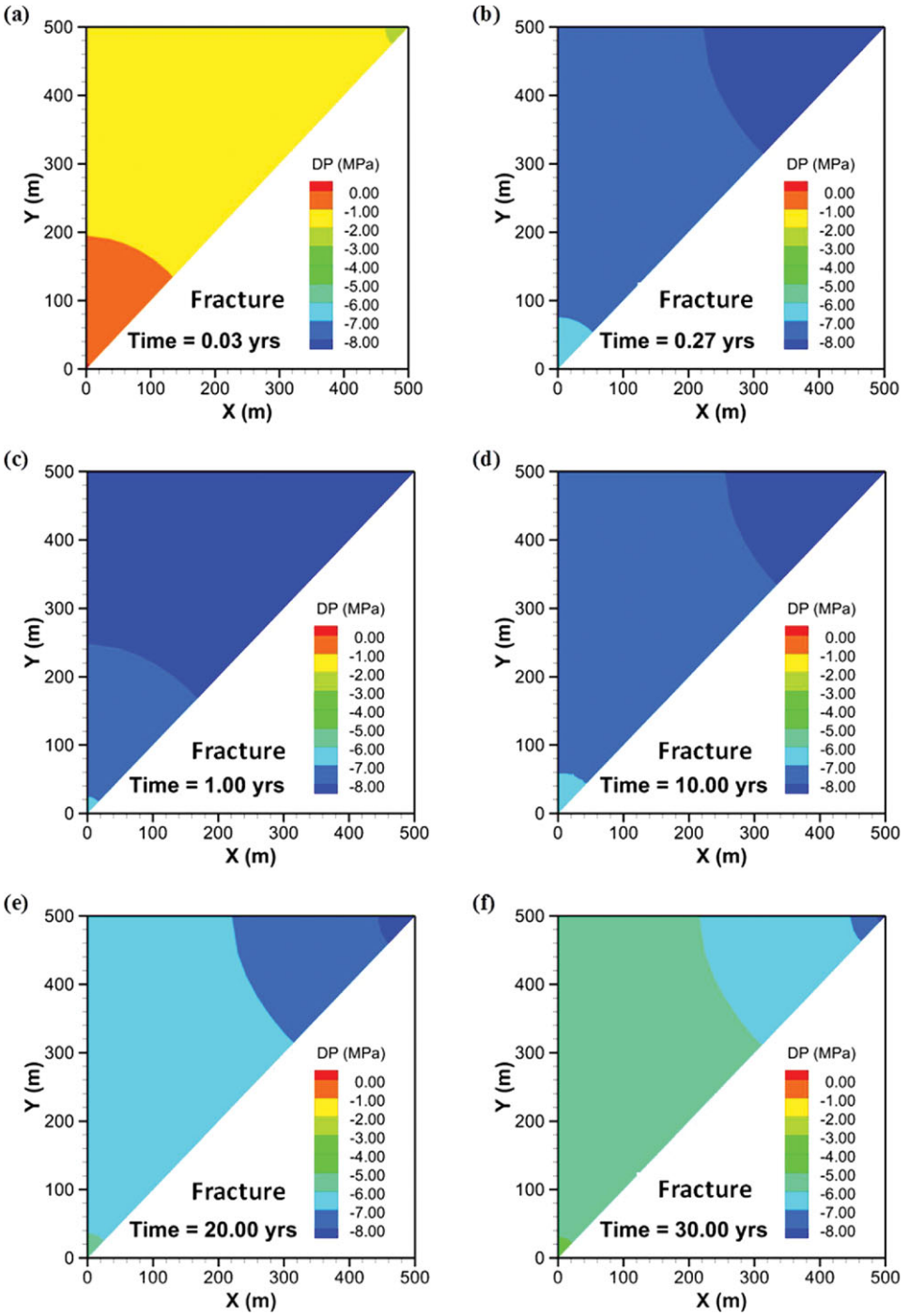

Figure 11. Simulated pressure drop (from the initial reservoir pressure) in the reservoir (a) 10 days, (b) 100 days, (c) 1 yrs, (d) 10 yrs, (e) 20 yrs, and (f) 30yrs.

salt. The code represents thermophysical properties of brine-CO_2 mixtures generally within experimental accuracy for the range of conditions of interest in geologic disposal of CO_2 and CO_2 enhanced geothermal reservoirs. Supercritical as well as subcritical conditions may be modeled, but the code currently has no provisions to treat separate liquid and gas CO2 phases, or transitions between them.

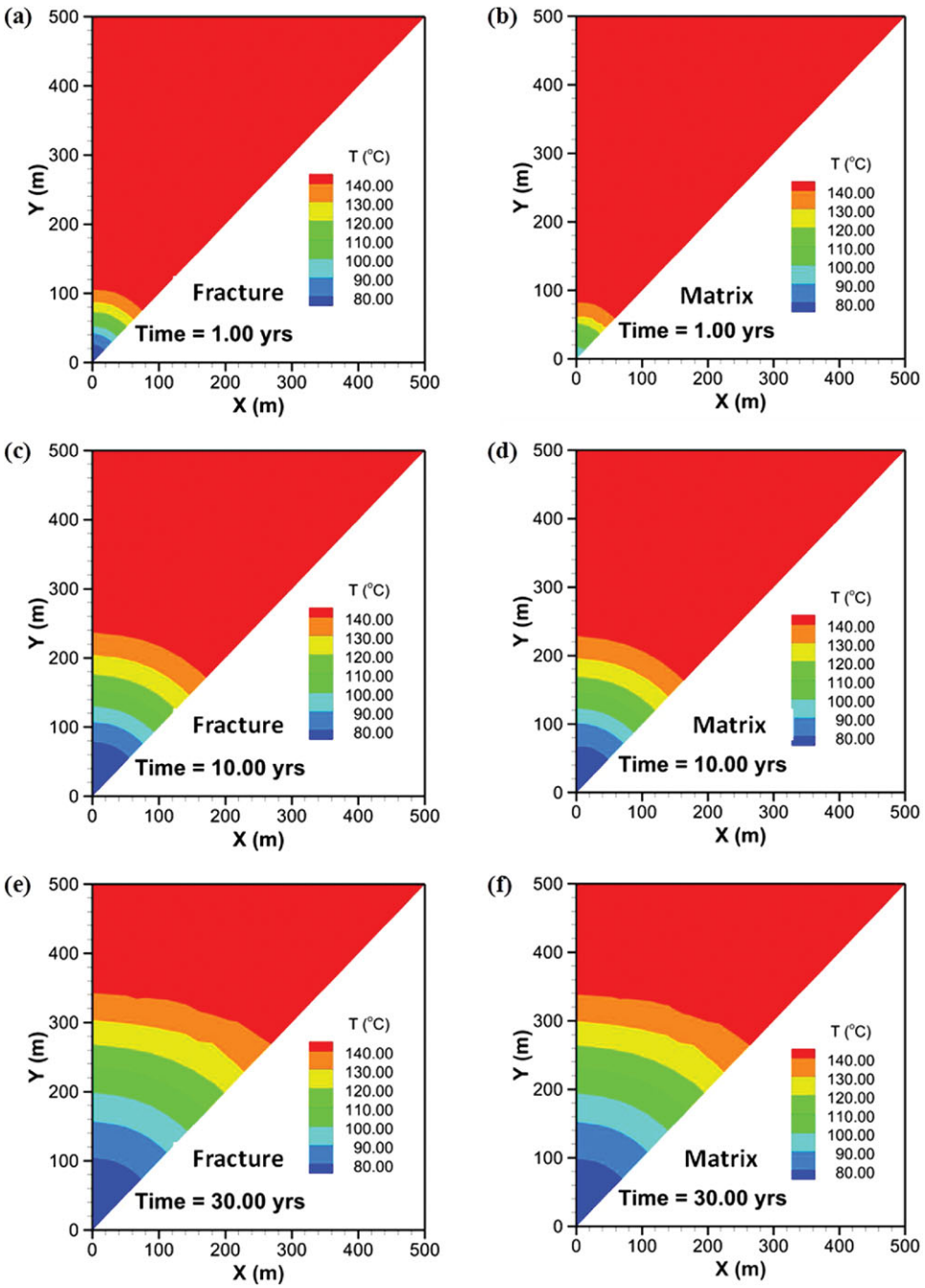

Figure 12. Simulated temperature in the reservoir after 1 year ((a) and (b)), 10 years ((c) and (d)), and 30 years ((e) and (f)) in the two continua.

Acknowledgments

This work was partly supported by the TOUGH Royalty Fund, the Director, Office of Science, Office of Basic Energy Sciences of the US Department of Energy, and by the Zero Emission Research and Technology project (ZERT) under Contract No. DE-AC03-76SF00098, and the Assistant Secretary for Energy Efficiency and Renewable Energy, Geothermal Technologies Program of the US Department of Energy under Contract No. DE-AC02-05CH11231.

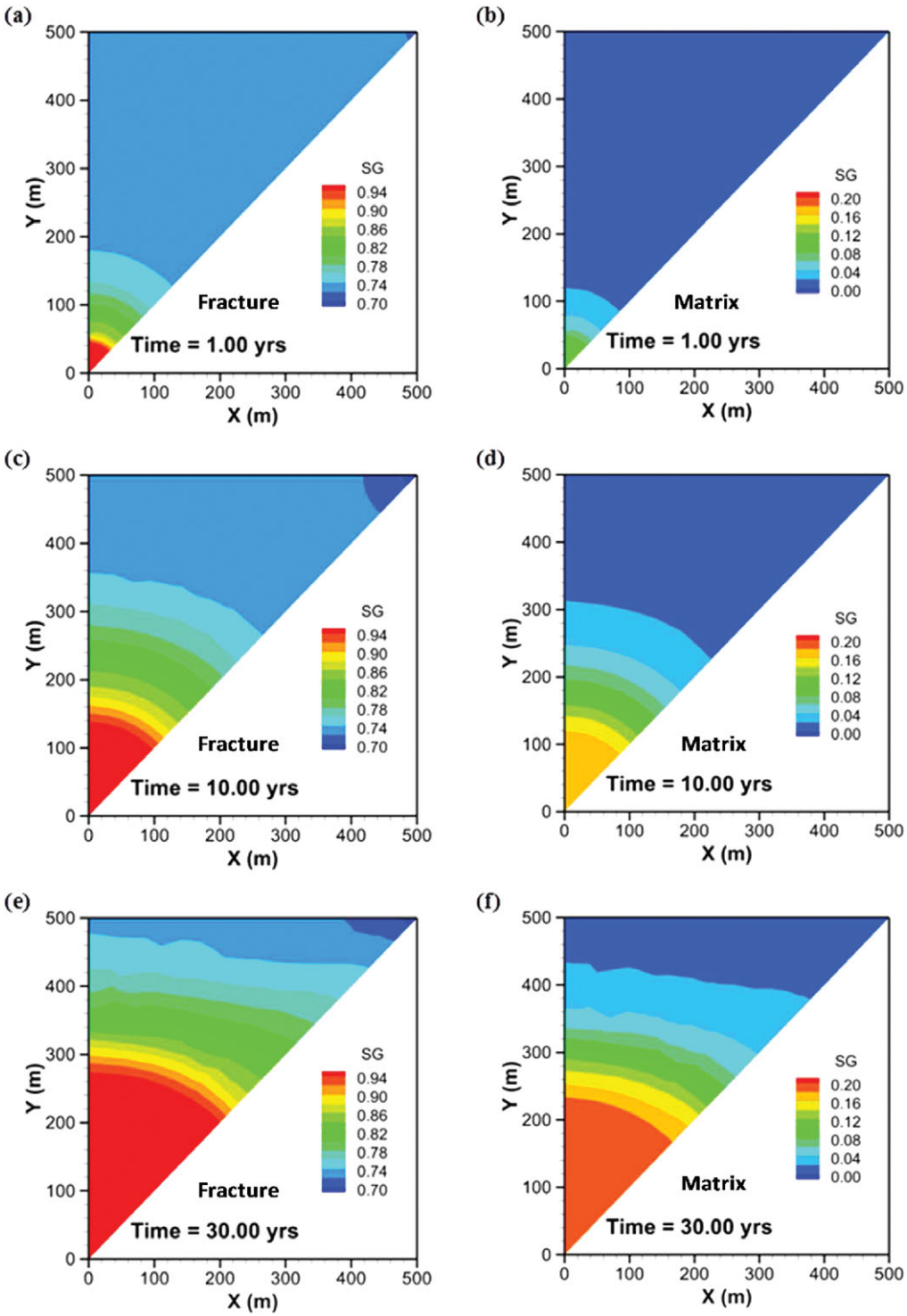

Figure 13. Simulated gas saturation in the reservoir after 1 year ((a) and (b)), 10 years ((c) and (d)), and 30 years ((e) and (f)) in the two continua. Different color scales are used for each continuum.

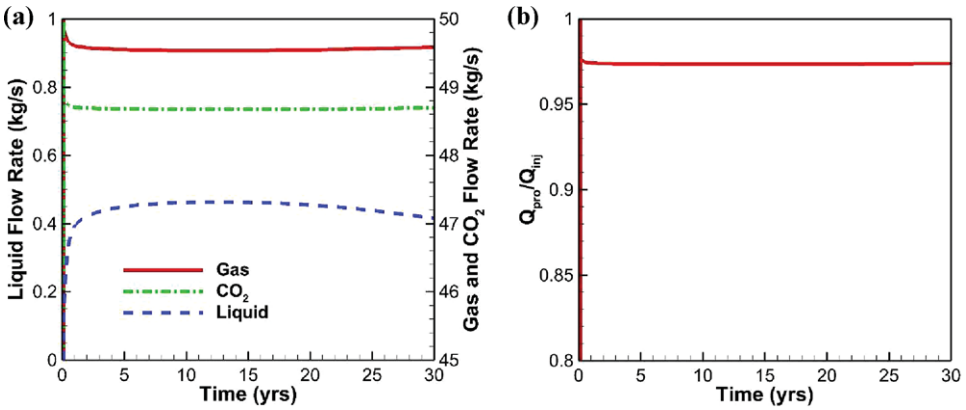

Figure 14. (a) Simulated gas and liquid phase flow rates as well as CO_2 component flow rate and (b) Ratio of CO_2 injection rate and production rate. Because the total injection (pure CO_2) rate and the total production (mixture) rate are equal, this ratio is also a measure of how much CO_2 enters the production stream.

References

1. Pruess K, The TOUGH codes – A family of simulation tools for multiphase flow and transport processes in permeable media. *Vadose Zone J* **3**:738–746 (2004).
2. Pruess K, ECO2N: A TOUGH2 fluid property module for mixtures of water, NaCl, and CO_2. Lawrence Berkeley National Laboratory Report LBNL-57952. Lawrence Berkeley National Laboratory, Berkeley, CA (2005).
3. Pruess K, Oldenburg C and Moridis G, TOUGH2 user's guide, version 2. Lawrence Berkeley National Laboratory Report LBNL-43134. Lawrence Berkeley National Laboratory, Berkeley, CA November 1999, revised (2012).
4. Pruess K and Spycher N, ECO2N – A fluid property module for the TOUGH2 code for studies of CO_2 storage in saline aquifers. *Energ Convers Manage* **48(6)**:1761–1767 (2007).
5. Spycher N and Pruess K, A phase partitioning model for CO_2-brine mixtures at elevated temperatures and pressures: Application to CO_2-enhanced geothermal systems. *Transp Porous Med*. **82**:173–196 (2010).
6. Spycher N and Pruess K, CO_2-H_2O mixtures in the geological sequestration of CO_2. II. Partitioning in chloride brines at 12–100°C and up to 600 bar. *Geochim Cosmochim Acta* **69(**13**)**:3309–3320 (2005).
7. Pruess K, Integrated modeling of CO_2 storage and leakage scenarios including transitions between super- and subcritical conditions, and phase change between liquid and gaseous CO_2. *Greenhouse Gas Sci Technol* **1**:237–247 (2011).
8. Spycher N and Pruess K, A model for thermophysical properties of CO_2-brine mixtures at elevated temperatures and pressures. *Thirty-Sixth Workshop on Geothermal Reservoir Engineering*, Stanford University, Stanford, California, January 31–February 2 (2011).
9. Fenghour A and Wakeham W, Densities of (water + carbon dioxide) in the temperature range 415 K to 700 K and pressures up to 35 MPa. *J Chem Thermodynamics* **28**:433–446 (1996).
10. Patel MR, Holste JC, Hall KR and Eubank PT, Thermophysical properties of gaseous carbon dioxide-water mixtures. *Fluid Phase Equilibria* **36**:279–299 (1987).
11. Patel MR and Eubank PT, Experimental densities and derived thermodynamic properties for carbon dioxide-water mixtures. *J Chem Eng Data* **33(2)**:185–193 (1988).
12. Zawisza A and Maleslnska BY, Solubility of carbon dioxide in liquid water and of water in gaseous carbon dioxide in the range 0.2-5 MPa and at temperatures up to 473 K. *J Chem Eng Data* **20(4)**:288–391 (1981).
13. Zakirov IV, The P-V-T relations in the H_2O-CO_2 system at 300 and 400°C. *Geochem Intl* **21**:13–20 (1984).
14. Bottini SB and Saville G, Excess enthalpies for (water + itrogen)(g) and (water + carbon dioxide)(g) at 520 to 620 K and up to 4.5 MPa. *J Chem Thermodynamics* **17**:83–97 (1985).
15. Wormald CJ, Lancaster NM and Sellars AJ, The excess molar enthalpies of {xH_2O+(l -x)CO}(g) and {xH_2O+(l - x)CO_2}(g) at high temperatures and pressures. *J Chem Thermodynamics* **18**:135–147 (1986).
16. Davidson TA, A simple and accurate method for calculating viscosity of gaseous mixtures. Bureau of Mines, US Department of the Interior, Report of Investigations 9456 (1993).
17. Altunin VV, *Thermophysical properties of carbon dioxide (in Russian)*. Publishing House of Standards, Moscow, 551 pp. (1975).
18. Scalabrin G, Marchi P, Finezzo F and Span R, A reference multiparameter thermal conductivity equation for carbon dioxide with an optimized functional form. *J Phys Chem Ref Data* **35(4)**:1549–1575 (2006).
19. Powell RW, Thermal conductivities and expansion coefficients of water and ice. *Advances in Physics* **7(26)**:276–297 (1958).
20. Sharqawy MH, New correlations for seawater and pure water thermal conductivity at different temperatures and salinities. *Desalination* **313**:97–104 (2013).
21. Zimmerman RW, Thermal conductivity of fluid saturated rocks. *J Petrol Sci Eng* **3**:219–227 (1989).
22. Pan L, Spycher N, Doughty C and Pruess K, ECO2N V2.0: A TOUGH2 fluid property module for mixtures of water, NaCl, and CO_2. Lawrence Berkeley National Laboratory Report LBNL-6930E. Lawrence Berkeley National Laboratory, Berkeley, CA (2015).

23. Pruess K, García J, Kovscek T, Oldenburg C, Rutqvist J, Steefel C and Xu T, Intercomparison of numerical simulation codes for geologic disposal of CO_2. Lawrence Berkeley National Laboratory Report LBNL-51813. Lawrence Berkeley National Laboratory, Berkeley, CA (2002).
24. Pruess K, García J, Kovscek T, Oldenburg C, Rutqvist J, Steefel C and Xu T, Code intercomparison builds confidence in numerical simulation models for geologic disposal of CO_2. *Energy* **29(**9-10**)**:1431–1444 (2004).
25. O'Sullivan MJ, A similarity method for geothermal well test analysis. *Water Resour Res* **17(**2**)**:390–398 (1981).
26. Warren JE and Root PJ, The behavior of naturally fractured reservoirs. *Soc Petrol Eng J Trans AIME* **228**:245–255 (1963).
27. van Genuchten MTh, A closed-form equation for predicting the hydraulic conductivity of unsaturated soils. *Soil Sci Soc Am J* **44**:892–898 (1980).
28. Corey AT, The interrelation between gas and oil relative permeabilities. *Producers Monthly* **19(**1**)**:38–41 (1954).
29. Vinsome PKW and Westerveld J, A simple method for predicting cap and base rock heat losses in thermal reservoir simulators. *J Canadian Pet Tech* **19(**3**)**:87–90 (1980).

Lehua Pan

Dr Lehua Pan has been working at Lawrence Berkeley National Laboratory since 1997 and is an expert in computer modeling of Earth systems and processes. He received his PhD in Soil Physics/Hydrology from University of Arizona in 1995, his MSc in Soil Physics from Zhejiang Agricultural University in 1986, and his BSc in Geology from Zhejiang University in 1982.

Nicolas Spycher

Nicolas Spycher has over twenty years' research experience in aqueous geochemistry and water/rock/gas interactions, including development of multicomponent geochemical and reactive transport models. His current research focuses on developing biogeochemical conceptual and numerical models to understand water/gas/rock/sediment interactions in the subsurface.

Christine Doughty

Christine Doughty is a staff scientist at Lawrence Berkeley National Laboratory. Her research interests include mathematical modeling of multi-component, multi-phase fluid flow and heat transport in heterogeneous geologic settings, including fractured rock. She obtained a PhD in Hydrogeology from the University of California, Berkeley in 1995.

Karsten Pruess

Karsten Pruess is a senior scientist emeritus of the Lawrence Berkeley National Laboratory, which he joined in 1977. He has conducted research in multiphase, non-isothermal, and chemically reactive flows in porous media, including mathematical modeling, analysis of field data, and laboratory experiments. He received a PhD in Physics from the University of Frankfurt, Germany in 1972.

